CHAPTER X

EVOLUTIONARY FRACTIONAL ORDER CONTROL OF A HUMANOID ROBOT MODELED AS A TRIPLE INVERTED PENDULUM

M. GONZÁLEZ-FIERRO, C. A. MONJE, C. BALAGUER[1]

[1]Robotics Lab, Universidad Carlos III de Madrid

This paper addresses the problem of robust control of a humanoid robot modeled as a triple inverted pendulum. Reduced models have the advantage of simplifying the complexity of the equations relating the variables involved in the dynamics of the robot, but have the drawback of mismatching with respect to the real complete model. Many researchers have proposed different control strategies for reduced models, but still an important effort is needed to be devoted to the problem of how this simplification affects the control performance. In this paper, we propose the use of a fractional order controller for the control of the humanoid, which is robust to changes in the model parameters. In particular, we have modeled a humanoid robot as an inverted triple pendulum, comparing the performance of a classical PID controller with a fractional order one when the pendulum masses change. We have tuned the controller parameters using differential evolution. The results are discussed in this paper, highlighting the robust performance obtained with the fractional order controller.

1 Introduction

In recent years there have been a strong discussion between researchers on favor to use mass distributed models to model a humanoid robot, where the mass and inertia of every link is known, and those who prefer to use a simplified or concentrated mass model, where all robot dynamics are simplified and concentrated in the center of gravity (Arbulú, 2009).

Those who prefer the representation of a complete dynamic representation defends that it allows more complex behavior, the model is more accurate and there is no need of complex control methods. In (Khatib, 2008) the authors perform a whole-body motion hierarchically dividing the control in tasks. Arbulu et al. (Arbulú, 2010) used Lie algebra to obtain the humanoid whole-body dynamics and reduce the computation time. In (Kajita, 2003) humanoid motion is accomplish controlling the momentum of a complete body model.

Many researchers make use of reduced dynamic models to control humanoids, some examples are the 2D and 3D linear inverted pendulum (LIPM) (Kajita, 1991; Kajita, 2001), cart-table (Kajita, 2003) or the angular momentum pendulum model (Komura, 2005).

A reduced model does not cover all dynamic behavior and non linearities of the real model, however, they are commonly used and many researchers have obtained good experimental results. In (Kaynov, 2009) a humanoid robot is modeled as a double inverted pendulum and a stabilizer is studied. (Mistry, 2010) models a humanoid as an inverted pendulum of five links and a stand up task is performed. Other examples can be found in (Kim, 2007). In (Pan, 2004) a triple inverted pendulum is controlled using an evolutionary approach. Another examples of triple pendulum control use H∞ (Tsachouridis, 1999) or fuzzy methods (Xiaofeng, 2009).

On the other hand, nowadays, the better understanding of the potential of fractional calculus and the increasing number of studies related to the applications of fractional order controllers in many areas of science and engineering have led to the importance of studying aspects such as the analysis, design, tuning and implementation of these controllers.

Fractional calculus (FC) is a generalization of the integration and differentiation to the non-integer (fractional) order fundamental operator D, where a and t are the limits and α ($\alpha \in \mathbb{R}$) is the order of the operation. Among many different definitions, two commonly used for the general fractional integro-differential operation are the Grünwald-Letnikov (GL) definition and the Riemann-Liouville (RL) definition (Podlubny, 1999). The GL definition is

$$ {}_a\mathrm{D}_t^{\alpha} f(t) = \lim_{h \to 0} h^{-\alpha} \sum_{j=0}^{[\frac{t-a}{h}]} (-1)^j \binom{\alpha}{j} f(t - jh) \tag{1} $$

where [·] means the integer part, while the RL definition is

$$ {}_a\mathrm{D}_t^{\alpha} f(t) = \frac{1}{\Gamma(n-\alpha)} \frac{\mathrm{d}^n}{\mathrm{d}t^n} \int_a^t \frac{f(\tau)}{(t-\tau)^{\alpha-n+1}} \mathrm{d}\tau \tag{2} $$

for (n-1 < α < n) and where Γ(·) is the *Euler's gamma* function.

For convenience, Laplace domain notion is commonly used to describe the fractional integro-differential operation. The Laplace transform of the RL fractional derivative/integral (2) under zero initial conditions for order α (0 < α < 1) is given by

$$ £\{ {}_a\mathrm{D}_t^{\pm\alpha} f(t)\} = s^{\pm\alpha} F(s) \tag{3} $$

In theory, control systems can include both the fractional order dynamic system to be controlled and the fractional order controller. However, in control practice, more common is to consider the fractional order controller. This is due to the fact that the system model may have been already obtained as an integer order model in the classical sense.

In this line, the objective of this work is to apply a fractional order control (FOC) strategy for the control of a humanoid robot modeled as a triple inverted pendulum, introducing a fractional order controller to improve the system performance and overtake the mismatches produced between the simplified and real models of the robot.

To test the robustness of our controller, we have compared a classical PID controller with a fractional controller when the humanoid follows a trajectory of standing up from a chair. We have overloaded the system adding 1 Kg. to every pendulum link, with the objective of evaluating the robot performance when there is a change in the mass of the model. The controller gains have been optimized with Differential Evolution.

The rest of the paper is organized as follows. Section II presents the simplified model of the HOAP humanoid robot as a triple inverted pendu-

lum, together with its state space representation. Section III gives a brief review on fractional order controllers and their implementation. Section IV introduces the differential evolution method used here to tune the different controllers proposed. In Section V, the simulation results are given and discussed, concluding in Section VI with the main conclusions and future works.

2 Reduced robot model

In a very simplified way, a humanoid robot can be dynamically modeled as a triple inverted pendulum. As it can be seen in Fig. 1 (Left), we have modeled the HOAP humanoid robot as a triple pendulum, where the ankle joint of the robot corresponds to the first pendulum joint, the knee joint corresponds to the second one, and the hip joint corresponds to the third one (see Fig. 1 (Right)).

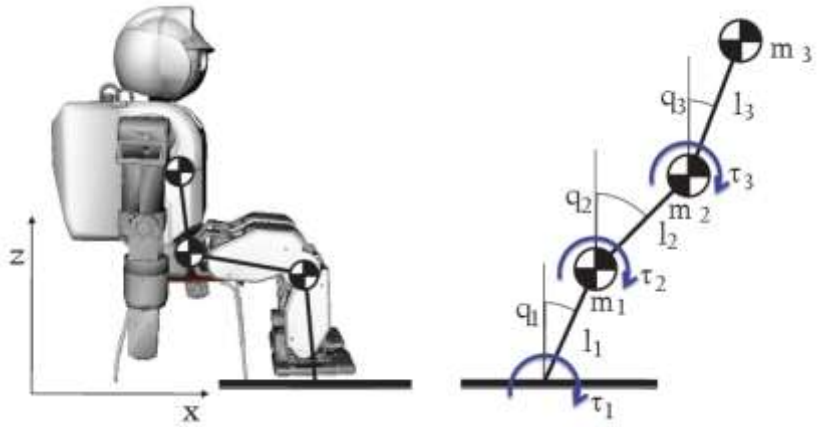

Fig. 1: Left: Reduced model of HOAP humanoid robot sited on a chair. The proposed model is a two dimensional triple inverted pendulum with massless links and the center of mass at the tip of the pendulum. Right: Triple inverted pendulum with masses, lengths, torques and positions.

The similarity is stated under the assumptions that the pendulum masses are concentrated at the tip of every link and the link masses are negligible. The control action that allows every mass m_i to move a position q_i is the torque τ_i.

Since the task we wanted to simulate is a robot standing up from a chair, we have chosen a triple pendulum to model the humanoid. The reason why we decided this is because there is a direct mapping between the pendulum joints and the joints needed for the robot to stand up. It is a good trade between selecting a simple inverted pendulum model and a complete model.

2.1 Triple pendulum equations

To obtain the triple pendulum equations let us define the position and velocity of every link.

$$x_1 = l_1 \sin q_1, \dot{x}_1 = l_1 \cos q_1 \dot{q}_1 \tag{4}$$

$$z_1 = l_1 \cos q_1, \dot{z}_1 = -l_1 \sin q_1 \dot{q}_1 \tag{5}$$

$$x_2 = l_1 \sin q_1 + l_2 \sin q_2 \tag{6}$$

$$\dot{x}_2 = l_1 \cos q_1 \dot{q}_1 + l_2 \cos q_2 \dot{q}_2 \tag{7}$$

$$z_2 = l_1 \cos q_1 + l_2 \cos q_2 \tag{8}$$

$$\dot{z}_2 = -l_1 \sin q_1 \dot{q}_1 - l_2 \sin q_2 \dot{q}_2 \tag{9}$$

$$x_3 = l_1 \sin q_1 + l_2 \sin q_2 + l_3 \sin q_3 \tag{10}$$

$$\dot{x}_3 = l_1 \cos q_1 \dot{q}_1 + l_2 \cos q_2 \dot{q}_2 + l_3 \cos q_3 \dot{q}_3 \tag{11}$$

$$z_3 = l_1 \cos q_1 + l_2 \cos q_2 + l_3 \cos q_3 \tag{12}$$

$$\dot{z}_3 = -l_1 \sin q_1 \dot{q}_1 - l_2 \sin q_2 \dot{q}_2 - l_3 \sin q_3 \dot{q}_3 \tag{13}$$

Articulated torques can be derived using the lagrangian equation:

$$\frac{d}{dt}\left(\frac{\partial \mathcal{L}}{\partial \dot{q}_i}\right) - \frac{\partial \mathcal{L}}{\partial q_i} = \tau_i \tag{14}$$

where the Lagrangian is the difference between kinetic and potential energy.

$$\mathcal{L} = \mathcal{T} - \mathcal{V} \tag{15}$$

$$\mathcal{V} = m_1 g z_1 + m_2 g z_2 + m_3 g z_3 \tag{16}$$

$$\mathcal{T} = \frac{1}{2} m_1 v_1^2 + \frac{1}{2} m_2 v_2^2 + \frac{1}{2} m_3 v_3^2 \tag{17}$$

where v_1, v_2 and v_3 are the speed of the centers of mass of the inverted pendulum with $v_i^2 = \dot{x}_i^2 + \dot{z}_i^2$. Substituting (4, …, 13) into (16) and (17) and then into (15), we obtain the equation of motion of the triple pendulum, whose compact form is stated as follows.

$$\tau = \mathbf{H}(\mathbf{q})\ddot{\mathbf{q}} + \mathbf{C}(\mathbf{q}, \dot{\mathbf{q}})\dot{\mathbf{q}} + \mathbf{G}(\mathbf{q}) \tag{18}$$

where $\boldsymbol{H} \in \mathbb{R}^{3x3}$ is the inertia matrix, $\boldsymbol{C} \in \mathbb{R}^{3x3}$ is the matrix of centrifugal and coriolis forces and $\boldsymbol{G} \in \mathbb{R}^{3x1}$ is the gravity matrix. The components of every matrix can be expressed as:

$$\begin{pmatrix} \tau_1 \\ \tau_2 \\ \tau_3 \end{pmatrix} = \begin{pmatrix} h_{11} & h_{12} & h_{13} \\ h_{21} & h_{22} & h_{23} \\ h_{31} & h_{32} & h_{33} \end{pmatrix} \begin{pmatrix} \ddot{q}_1 \\ \ddot{q}_2 \\ \ddot{q}_3 \end{pmatrix} + \begin{pmatrix} 0 & c_{12} & c_{13} \\ c_{21} & 0 & c_{23} \\ c_{31} & c_{32} & 0 \end{pmatrix} \begin{pmatrix} \dot{q}_1^2 \\ \dot{q}_2^2 \\ \dot{q}_3^2 \end{pmatrix} + \begin{pmatrix} g_1 \\ g_2 \\ g_3 \end{pmatrix} \tag{19}$$

$$h_{11} = l_1^{\,2}\left(m_1 + m_2 + m_3\right) \tag{20}$$

$$h_{22} = l_2^{\,2}\left(m_2 + m_3\right) \tag{21}$$

$$h_{33} = l_3^{\,2} m_3 \tag{22}$$

$$h_{12} = h_{21} = (m_2 + m_3) l_1 l_2 cos(q_1 - q_2) \tag{23}$$

$$h_{13} = h_{31} = m_3 l_1 l_3 cos(q_1 - q_3) \tag{24}$$

$$h_{23} = h_{32} = m_3 l_2 l_3 cos(q_2 - q_3) \tag{25}$$

$$c_{12} = -c_{21} = -(m_2 + m_3) l_1 l_2 sin(q_2 - q_1) \tag{26}$$

$$c_{13} = -c_{31} = -m_3 l_1 l_3 sin(q_3 - q_1) \tag{27}$$

$$c_{23} = -c_{32} = -m_3 l_2 l_3 sin(q_3 - q_2) \tag{28}$$

$$g_1 = -g l_1 \left(m_1 + m_2 + m_3\right) \sin\left(q_1\right) \tag{29}$$

$$g_2 = -g l_2 \left(m_2 + m_3\right) \sin\left(q_2\right) \tag{30}$$

$$g_3 = -g l_3 m_3 \sin\left(q_3\right) \tag{31}$$

2.2 State space representation of the triple pendulum

The inverted triple pendulum can be expressed as a dynamical system in the standard form:

$$\dot{X} = AX + BU, \quad Y = CX \tag{32}$$

where X is the state vector, U is the control vector and Y is the output vector. To obtain the representation of the triple pendulum system let us define the following state variables: $X_1 = q_1, X_2 = \dot{q}_1, X_3 = q_2, X_4 = q_2,$ $X_5 = q_3, X_6 = \dot{q}_3$

Taking this into account, and reordering (18), the matrices A, B and C can be obtained knowing that:

$$\dot{X}_1 = X_2, \dot{X}_3 = X_4, \dot{X}_5 = X_6 \tag{33}$$

$$\begin{pmatrix} \dot{X}_2 \\ \dot{X}_4 \\ \dot{X}_6 \end{pmatrix} = \hat{f}(X_1, X_2, X_3, X_4, X_5, X_6) \tag{34}$$

Where $\hat{f}$ contains nonlinear terms of the state variables.

To avoid the nonlinear terms, we have linearized over X_{i0} using a Taylor expansion:

$$\dot{\tilde{X}} = A\tilde{X} + B\tilde{U} \tag{35}$$

$$A = \frac{\partial f}{\partial X}\Big|_{\substack{X=X_0 \\ U=U_0}} \quad ; \quad B = \frac{\partial f}{\partial U}\Big|_{\substack{X=X_0 \\ U=U_0}} \tag{36}$$

and $\tilde{X}_i = X_i - X_{i0}$.

Since the desired trajectory has a wide variation, we have selected three regions of linearization, obtaining three subsystems. We have divided the desired trajectory in three regions and we have chosen the middle point of every region as the linearization point. In Fig. 2 the selected linearization

positions are shown. The result is three linear systems that are going to be controlled with standard and fractional order PID controllers using the Differential Evolution approach, as will be explained later.

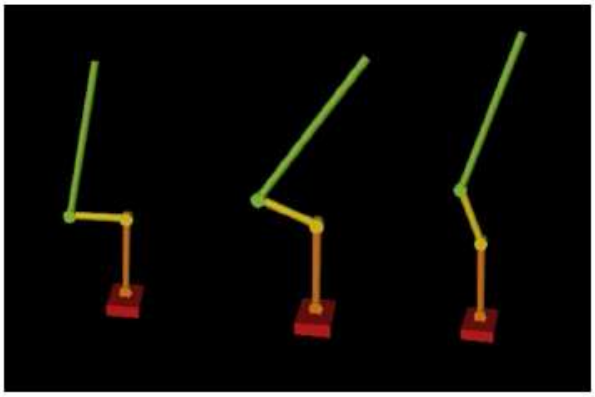

Fig. 2: The three positions of the system linearization. Every position is a point of linearization and defines a linear system.

3 Fractional order controllers

This section presents the main features of the fractional order controllers and it implementation.

3.1 A brief review

The theoretical and practical interest of fractional order operators is nowadays well established, and its applicability to science and engineering can be considered as an emerging new topic. Even if they can be thought of as somehow ideal, they are, in fact, useful tools for both the description of a more complex reality and the enlargement of the practical applicability of the common integer order operators. Among these fractional order operators and operations, the fractional integro-differential operators (fractional calculus) are specially interesting in automatic control and robotics, among others.

Going a step further in automatic control, (Oustaloup, 2000) studied the fractional order algorithms for the control of dynamic systems and demonstrated the superior performance of the CRONE (Commande Robuste d'Ordre Non Entier) method over the PID controller. (Podlubny, 1999) proposed a generalization of the PID controller, namely the $PI^{\lambda}D^{\mu}$ controller, involving an integrator of order $%\lambda $ and a differentiator of order $\mu .$ He also demonstrated the better response of this type of controller, in comparison with the classical PID controller, when used for the control of fractional order systems. A frequency domain approach by using fractional order PID controllers has also been studied in (Monje, 2010).

Fractional calculus also extends to other kinds of control strategies different from PID ones, but in the case study presented in this paper we propose the use of the fractional order $PI^{\lambda}D^{\mu}$ controller as a robust alternative for the control of a humanoid robot simplified model based on the triple inverted pendulum. More details will be given later.

3.2 Implementation

Before introducing the differential evolution method used for the tuning of the different controllers proposed in this paper, some considerations on the implementation of the fractional order $PI^{\lambda}D^{\mu}$ controller have to be taken into account. A very good review regarding this topic is given in (Monje, 2010).

The generalized transfer function of this controller is given by

$$c(s) = k_p + \frac{k_i}{s^{\lambda}} + k_d s^{\mu} \tag{37}$$

In general, when fractional order controllers have to be implemented or simulations have to be performed, fractional transfer functions are usually replaced by integer transfer functions with a behavior close enough to the one desired, but much easier to handle. There are many different ways of finding such approximations but unfortunately it is not possible to say that one of them is the best, because even though some of them are better than others in regard to certain characteristics, the relative merits of each approximation depend on the differentiation order, on whether one is more

interested in an accurate frequency behavior or in accurate time responses, on how large admissible transfer functions may be, and other factors like these (Monje, 2010).

In this work a frequency identification method performed by the Matlab function *invfreqs* (Monje, 2010) has been used. With this method a rational transfer function is obtained whose frequency response fits the frequency response of the original irrational transfer function within a selected frequency range. This method is chosen due to its accuracy in the frequency range of interest, which can be adjusted by selecting the number of poles/zeros of the rational transfer function.

4 Differential Evolution

Differential Evolution (DE) is a stochastic search optimization method based on genetic algorithms (Storn, 1997). It is widely used in SLAM (Moreno, 2009), multiobjective optimization (Xue, 2003), pattern recognition (Bueno, 2012) or constraint optimization (Huang, 2007).

This algorithm selects a random initial population over a bounded domain $x_{\min}$ and $x_{\max}$, generating N population members. Similarly to another evolutionary algorithms, it perturbs the population, generating new members that are going to be evaluated in a fitness function.

The selection and combination of new points are randomly chosen from three individuals. Two of the members, x_{r1} and x_{r2}, are subtracted and multiplied by a weight F, and then added to another x_{r3} giving a trial solution:

$$u_0 = x_{r3} + F(x_{r1} - x_{r2}) \tag{38}$$

This solution u_0 is evaluated in the fitness function and compared with the rest of the vector of the same index. This process is repeated until a population of N has competed against the trial solution randomly generated. Once the last vector has been evaluated, the best members are selected for the next iteration.

The computation ends when a final condition has been achieved. Usual conditions are time, number of iterations or a specific value of the fitness function.

In this paper we have used DE to optimize the values of the PID controller gains $k_p, k_i, k_d \in \mathbb{R}^{3x3}$ and the gains and orders of the fractional order controller k_p, k_i, k_d, λ and μ.

5 Results and discussion

This section present and discuss the results.

5.1 Identification of pendulum parameters

To obtain the triple inverted pendulum parameters a system identification was performed. For this purpose we used DE optimizer, computing a triple pendulum's Zero Moment Point (ZMP) trajectory and comparing it with the real ZMP measurement of the robot feet FSR sensors (Fig. 3), minimizing the quadratic difference.

The multibody ZMP equation in the sagital plane is

$$ZMP = \frac{\sum_{i=1}^{n} m_i x_i (\ddot{z}_i + g) - \sum_{i=1}^{n} m_i \ddot{x}_i z_i + \sum_{i=1}^{n} I_{iy} \alpha_{iy}}{\sum_{i=1}^{n} m_i (\ddot{z}_i + g)} \tag{39}$$

The reason why we used the ZMP to perform the identification is because ZMP is a measurement of stability, and we can obtain a real ZMP directly from robot sensors. This is more intuitive and gives more information than simple joint trajectories.

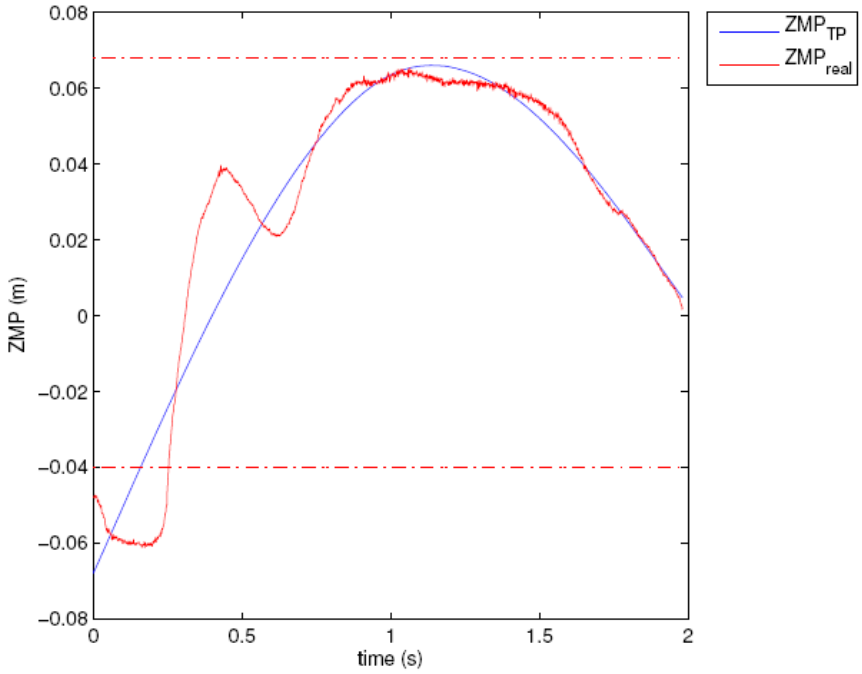

Fig. 3. ZMP trajectory of the triple inverted pendulum and ZMP of the real robot measured with the feet sensors.

Our identification is based on the work of (Tang, 2008). The results are shown in the Table 1.

Table 1: Triple pendulum identification parameters

	Mass (Kg)	Lenght (m)
Link 1	0.505	0.167
Link 2	0.500	0.260
Link 3	3.900	0.264

Taking these parameters into account and the three operating points previously stated (Fig. 2), we obtained three linearized subsystems using (35). Each subsystem was controlled using an standard and a fractional order PID controller, whose gains $k_p, k_i, k_d \in \mathbb{R}^{3x3}$ and fractional orders λ and μ,

have been obtained using DE. To change between systems, we used a gain scheduling strategy.

The desired trajectory has been manually defined using three order splines and it simulates a stand up trajectory. The trajectory has been divided into three regions of two seconds, corresponding to the three subsystems each. In Fig. 4 the simulated trajectory is shown.

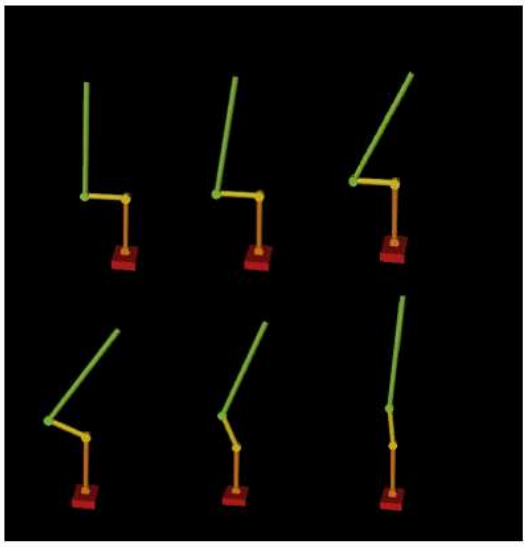

Fig 4. Simulation of triple inverted pendulum trajectory.

Furthermore, to estimate the controller robustness, we have overloaded the pendulum masses, adding 1 Kg to each link and comparing the new responses with those obtained from the nominal system.

5.2 Comparison between classical and fractional order controller

All simulations have been performed in MATLAB, using Runge-Kutta solver and a sampling time of 1 ms.

The differential evolution algorithm produces random values of the controller gains, whose are used to simulate the system in Fig. 5. The fitness function to minimize is the difference between the system output and the reference. The best member of every iteration is mutated and evaluated again until a final value of the fitness function is reached or a total number of iteration is passed. In our case, the final value is 1 and the maximum number of iterations is 50.

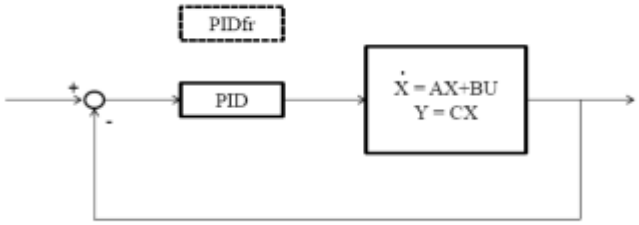

Fig. 5. Control system. The block PID is changed for the block PIDfr when the fractional order control strategy is used.

This is done for every subsystem with the standard PID gains and with the fractional order PID gains and λ and μ orders.

To approximate the behavior of a fractional controller, we have used the frequency identification method *invfreqs* provided by MATLAB. The chosen crossover frequency has been 0.001 rad/s and we approximated the behavior of the fractional controller for 4 decades.

The approximation of the fractional controller is a rational expression of order 8. This expression is evaluated in MATLAB and substituted in the block $PI^{\lambda}D^{\mu}$ of Fig. 5.

For the sake of space, we are just presenting the parameters of the fractional order PID controller for the first region, similarly obtaining the corresponding controllers for the other two regions, and so for the classical PID case.

$$k_{p1} = \begin{pmatrix} 404.727 & -305.224 & -782.663 \\ 1887.738 & -102.147 & -6281.782 \\ 1097.379 & -13.248 & 417.511 \end{pmatrix}$$

$$k_{i1} = \begin{pmatrix} -13129.120 & 13074.195 & -5581.229 \\ -1185.499 & -118.561 & 1321.581 \\ -1971.739 & -933.607 & 12007.290 \end{pmatrix}$$

$$k_{d1} = \begin{pmatrix} 10891.500 & 6320.620 & 1687.942 \\ -3646.421 & 1252.162 & 7721.200 \\ 1025.524 & -943.733 & -1851.324 \end{pmatrix}$$

$$\lambda_1 = 0.595; \mu_1 = -0.432$$

The results obtained for the three regions are presented in Fig. 6, Fig. 7 and Fig. 8, respectively.

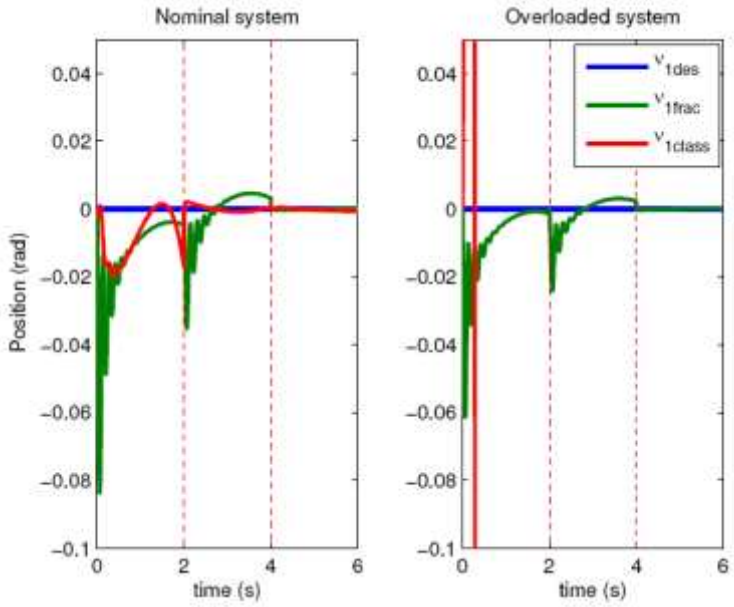

Fig. 6. System response for joint 1 for the nominal (left) and overloaded (right) subsystem. In blue is the desired trajectory, in green the trajectory with the fractional order controller and in green the trajectory with the standard PID. In dotted red the limits of the three linearization regions.

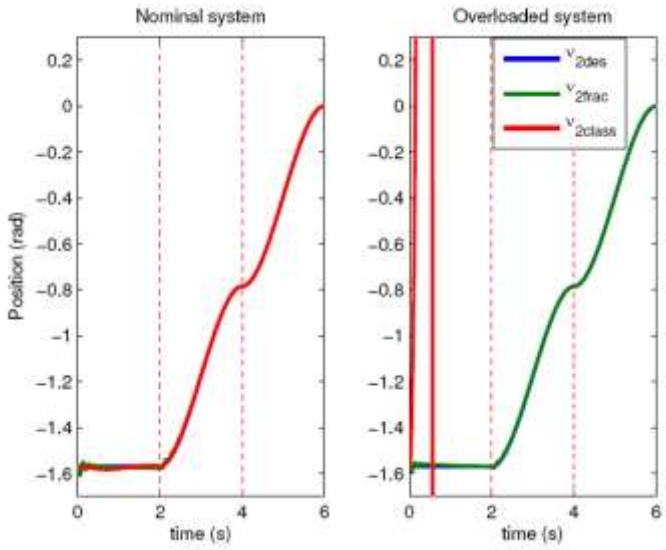

Fig. 7. System response for joint 2 for the nominal (left) and overloaded (right) subsystem.

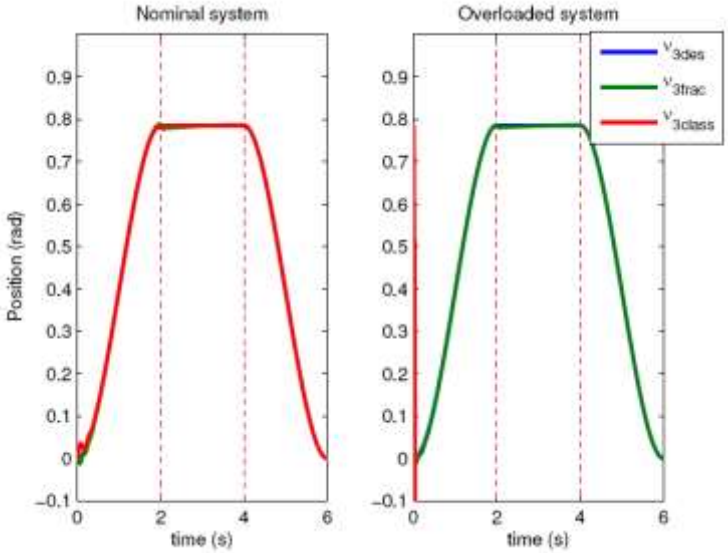

Fig. 8. System response for joint 3 for the nominal (left) and overloaded (right) subsystem.

As can be seen, the fractional order controller keeps the stability of the system in case a significant masses mismatch appears in the model. This way, we can guarantee the robustness of the control system to uncertainties in the model, compensating this way the effects of using for simplicity a reduced model of the robot for control purposes. On the contrary, the responses with the standard PID controller are unstable for some of the joins when the system is overloaded.

6 Conclusions

This paper addresses the problem of modeling and controlling a reduced model of a humanoid robot based on the triple inverted pendulum. A control technique that uses differential evolution and a fractional order PID controller is applied, obtaining very good results.

The effect of mass mismatches between the real and the simplified model of the humanoid is compensated to a significant extent by the fractional order PID controller, which ensure the robust response of the whole system during the whole motion when a mass increase of 1 Kg is considered in each tip.

After comparing the behavior of the humanoid when performing a standing up movement using the standard PID controller and the fractional order one, it is concluded that, using differential evolution as gain optimizer, both controllers track the reference satisfactorily for the nominal case. However, when the robot is overloaded, only the fractional order controller guarantee the stability of the system. We are currently working on testing this control strategy in the real humanoid.

References

Arbulu, M. (2009), *Stable locomotion of humanoid robots based on mass concentrated model*, Ph. D. Thesis.

Arbulú, M., Balaguer, C., Monge, C., Martínez, S., and Jardon, A. (2010), *Aiming for multibody dynamics on stable humanoid motion with special*

euclideans groups, IEEE/RSJ International Conference on Intelligent Robots and Systems (IROS), 691–697.

Bueno, J. G., M. González-Fierro, L.Moreno, and C.Balaguer (2012), *Facial Gesture Recognition using Active Appearance Models based on Neural Evolution,* International Conference on Human-Robot Interaction (HRI 2012).

Huang, F., Wang, L., and He, Q. (2007), *An effective co-evolutionary differential evolution for constrained optimization*, Applied Mathematics and computation 186(1), volume 186, Elsevier, 340–356.

Kajita, S., and Tani, K. (1991), *Study of dynamic biped locomotion on rugged terrain-theory and basic experiment*, ICAR, Fifth International Conference on Advanced Robotics, 1991.'Robots in Unstructured Environments', 741–746.

Kajita, S., Kanehiro, F., Kaneko, K., Yokoi, K., and Hirukawa, H. (2001), *The 3D Linear Inverted Pendulum Mode: A simple modeling for a biped walking pattern generation*, Proceedings of IEEE/RSJ International Conference on Intelligent Robots and Systems, volume 1, 239–246.

Kajita, S., Kanehiro, F., Kaneko, K., Fujiwara, K., Harada, K., Yokoi, K., and Hirukawa, H. (2003), *Biped walking pattern generation by using preview control of zero-moment point*, Proceedings of IEEE International Conference on Robotics and Automation, volume 2, 1620–1626, 2003

Kaynov, D., Soueres, P., Pierro, P., and Balaguer, C. (2009), *A practical decoupled stabilizer for joint-position controlled humanoid robots*, IEEE/RSJ International Conference on Intelligent Robots and Systems, IROS 2009, 3392–3397.

Khatib, O., Sentis, L., and Park, J.H. (2008), *A unified framework for whole-body humanoid robot control with multiple constraints and contacts*, European Robotics Symposium 2008, 303–312.

Kim, J.Y., Park, I.W., and Oh, J.H. (2007), *Walking control algorithm of biped humanoid robot on uneven and inclined floor*, Journal of Intelligent & Robotic Systems 48(4), volume 48, Springer, 457–484.

Komura, T., Leung, H., Kudoh, S., and Kuffner, J. (2005), *A feedback controller for biped humanoids that can counteract large perturbations during gait*, Proceedings of the 2005 IEEE International Conference on Robotics and Automation, ICRA 2005, 1989–1995.

Mistry, M., Murai, A., Yamane, K., and Hodgins, J. (2010), *Sit-to-stand task on a humanoid robot from human demonstration*, 10th IEEE-RAS International Conference on Humanoid Robots (Humanoids), 218–223.

Monje, C. A., Chen, Y. Q., Xue, D., Vinagre, B. M., and Feliu, V. (2010) *Fractional-order Systems and Controls. Fundamentals and Applications*, volume , Springer.

Moreno, L., Garrido, S., Blanco, D., and Muñoz, M.L. (2009) *Differential evolution solution to the SLAM problem*, Robotics and Autonomous Systems 57(4), volume 57, Elsevier, 441–450.

Oustaloup, A., Levron, F., Nanot, F., and Mathieu, B. (2000), *Frequency-band Complex Non Integer Differentiator: Characterization and Synthesis*, IEEE Transactions on Circuits and Systems 47(1), volume 47, 25–40.

Pan, W., Chengzhi, X., and Zhun, F. (2004), *Evolutionary linear control strategies of triple inverted pendulums and simulation studies*, Fifth World Congress on Intelligent Control and Automation. WCICA 2004, volume 3, 2365–236.

Podlubny, I. (1999) *Fractional-Order Systems and PID Controllers*, IEEE Transactions on Automatic Control 44(1), volume 44, 208–214.

Tsachouridis, V.A. (1999) *Robust control of a triple inverted pendulum*, Proceedings of the 1999 IEEE International Conference on Control Applications, volume 2, 1235–1240, 1999

Storn, R., and Price, K. (1997), *Differential evolution, a simple and efficient heuristic for global optimization over continuous spaces*, Journal of global optimization 11(4), volume 11, Springer, 341–359.

Tang, H., Xue, S., and Fan, C. (2008) *Differential evolution strategy for structural system identification*, Computers & Structures 86(21-22), volume 86, Elsevier, 2004–2012.

Xiaofeng, G., Hongxing, L., Guannan, D., and Haigang, G. (2009), *Variable universe adaptive fuzzy control on the triple inverted pendulum and choosing contraction-expansion factor*, International Conference on Artificial Intelligence and Computational Intelligence. AICI'09, volume 4, 63–67.

Xue, F., Sanderson, A.C., and Graves, R.J. (2003) *Pareto-based multi-objective differential evolution*, The 2003 Congress on Evolutionary Computation. CEC'03., volume 2, 862–869.